International Journal of Fluid Mechanics & Thermal Sciences
2022; 8(3): 53-63
http://www.sciencepublishinggroup.com/j/ijfmts
doi: 10.11648/j.ijfmts.20220803.12
ISSN: 2469-8105 (Print); ISSN: 2469-8113 (Online)

Study of Thermal Fields in a Semi - Ventilated Enclosure Heated by a Linear Heat Source

Koueni-Toko Christian Anicet

Department of Renewable Energy, National Advanced School of Engineering of Maroua, University of Maroua, Maroua, Cameroon

Email address:
christiandrkoueni@gmail.com

To cite this article:
Koueni-Toko Christian Anicet. Study of Thermal Fields in a Semi - Ventilated Enclosure Heated by a Linear Heat Source. *International Journal of Fluid Mechanics & Thermal Sciences*. Vol. 8, No. 3, 2022, pp. 53-63. doi: 10.11648/j.ijfmts.20220803.12

Received: July 19, 2022; **Accepted**: August 4, 2022; **Published**: August 10, 2022

Abstract: The objective of this work is to numerically study the temperature fields and to model the differential static pressure in a semi-ventilated enclosure heated by a linear heat source. The semi-ventilated enclosure has a height of 520 mm, a width of 210 mm and a length of 210 mm and has two openings located in the ceiling of the enclosure on the two side walls located at positions x + = - 0.5 and 0.5. The openings have a height of 34 mm and a length of 210 mm. The linear heat source has a diameter of 20 mm and a length of 200 mm and is placed in the position x + = 0 and 2 mm from the floor. Numerical calculations of thermal fields and differential static pressure were performed using the DNS method. The simulation technique is based on the finite volume method. The study was carried out in steady state. The discretization of the equations was carried out based on the QUICK scheme. This discretization gives a system of algebraic equations whose solution makes it possible to determine the fields of temperature and differential static pressure. The SIMPLE algorithm was used for pressure correction on a non-uniform mesh. The "Weighted Body Strength" scheme for pressure resolution. The results obtained show that the thermal plume slopes towards the right wall of the enclosure, reaches the ceiling where it is destroyed by shearing. Hot gases exit the enclosure at the top of the openings and cool air enters the enclosure from the bottom. The values of the differential static pressure at the openings are positive at the top where the hot gases exit and negative at the bottom where the fresh air enters the enclosure. Cool air descends to the bottom of the enclosure near the side walls and mixes with the warm air in the enclosure. The movements of air in the enclosure are governed by the thermal plume. The comparison of the differential static pressure obtained by numerical calculations with those of the experiments agrees.

Keywords: Semi-Ventilated Enclosure, Linear Heat Source, Thermal Fields, Differential Static Pressure

1. Introduction

Natural convection is created by movements of internal origin caused by the forces of Archimedes $\delta\overrightarrow{\rho g}$. These upward movements are due to the difference in density which is most of the time caused by the temperature difference with the force of gravity creates a buoyancy force which therefore creates a difference in momentum. The study of natural convection in enclosures with at least one opening can generate the movements of fluid at the level of the opening (s) [1-3]. In this situation we can speak of natural ventilation [4-10].

The study of natural ventilation in semi - confined enclosures has been the subject of a large number of theoretical, experimental and numerical works. In particular that of Linden, Lane-Serff and Smeed [1], who studied the case of a point source of buoyancy located at the bottom of an enclosure comprising two openings, one of which is located at the bottom and the other at the top, height H and radius R, with an aspect ratio $H / R < 1$. They showed that there is a displacement regime and that stratification develops characterized by two layers separated by an interface. Kaye and Hunt [2], studied the same type of situation in the case of a rectangular enclosure presenting a heat source located at the bottom of the enclosure and two openings located at the base and at the top. They have shown that the steady state depends on two times: the filling time and the emptying time. For aspect ratios of $1 < H / R < 5.8$, Kaye and Hunt [5], have shown that vortices appear near the walls and induce an increase in the quantity of air entering the enclosure which creates a thickening of the upper layer (layer at uniform temperature). Jeremy and Woods [8] investigated in laboratory experiments the transient filling of a room with buoyant fluid

when a doorway connects the room to a large reservoir of dense fluid. And shown that the filling time has the expression $(A/wH)\times(H/g')^{1/2}$. Fitzgerald and Woods [11] studied theoretically and experimentally the natural ventilation of a room with a heat source at the base and with vents at multiple heights. They showed through the determination of neutral buoyancy that air enters through the vents below the neutral buoyancy position and exits through the vents above. When a room is heated by a point source, a vertically stratified environment develops and the neutral buoyancy surface is higher than for a distributed source. To create the buoyancy force in semi-confined enclosures, previous authors who worked on natural ventilation used a fluid source in water or air. The following authors have used a solid hot source in air. This source of buoyancy can be point, linear [11, 12] or distributed [13] and located on the floor, on the ceiling on one of the side walls or inside the enclosure. Or the well-mixed hot gas enclosure initially [14]. The following authors used a solid, linear hot source, located close to the floor and centered.

Koueni Toko [2] carried out an experimental, analytical and numerical study of the temperature fields in an enclosure with two symmetrical openings located near the floor, heated by a cylindrical heat source (case 11). He showed that, when the temperature of the heat source takes constant values ΔT_0 = 40 K, 60 K and 75 K, a symmetrical thermal plume is observed in the steady state. It also showed the presence of air flows at each opening. These airflows consist of cool air entering at the bottom of the openings and hot gases exiting at the top.

Koueni *et al*. [3] studied Numerical modeling of the temperature fields in a semi-confined enclosure heated by a linear heat source. The enclosure has an aspect ratio H / L = 2.476 and twenty (20) openings located near the floor on two (02) side walls of height H and width l. Each side wall has ten (10) openings distributed over two (02) horizontal rows on the axis (0y) in equal number. The heat source is linear. They showed in steady state that the thermal plume was near-centered and the temperature values in the chamber increased as the reduced Rayleigh number increased. Considering the same configuration, Koueni Toko Christian Anicet [15] studied the velocity fields and modeled the differential static pressure profiles. He showed that at the level of the lower openings there is on each side wall a fresh air inlet and an outlet for the hot gases from the enclosure. It also shows that the values of the velocity in the enclosure increase with the reduced Rayleigh number.

Koueni Toko Christian Anicet et al. [16] experimentally studied the differential static pressure profiles in four enclosures (case 1, case 2, case 3 and case 4) with different opening positions. They showed that the differential static pressure profiles in each of these enclosures were different regardless of the values of the reduced Rayleigh number.

The interest of such studies lies in their implication in many industrial applications such as the cooling of electronic components, the heating of buildings, the fires of compartments, etc.

We will study by numerical calculation the temperature fields and the differential static pressure profiles generated in a rectangular enclosure with an aspect ratio H/L = 2.476, heated by a cylindrical heat source and comprising two openings near the ceiling located on each side wall. This enclosure (case 2) was made experimentally by Koueni Toko Christian Anicet et al. [16]. The experimental study of the differential static pressure profiles in this containment was carried out by Koueni Toko Christian Anicet et al. [16].

This study has never been performed.

The objective of this work is to understand and successfully control the phenomena found at the openings when the enclosure is subjected to a linear heat source. We will show the influence of the reduced Rayleigh number (Ra^*) on the numerical temperature fields, the numerical temperature difference and the numerical differential static pressure. This study will be carried out in steady state.

2. Numerical Device

The numerical device used for the numerical calculations is shown in Figure 1. The difference between this device and that of the experiment (case 2) [16] lies in the geometry of the heat source. In the experimental device (case 2) [16], the base section of the heat source is a circle while for the numerical device the base section is square.

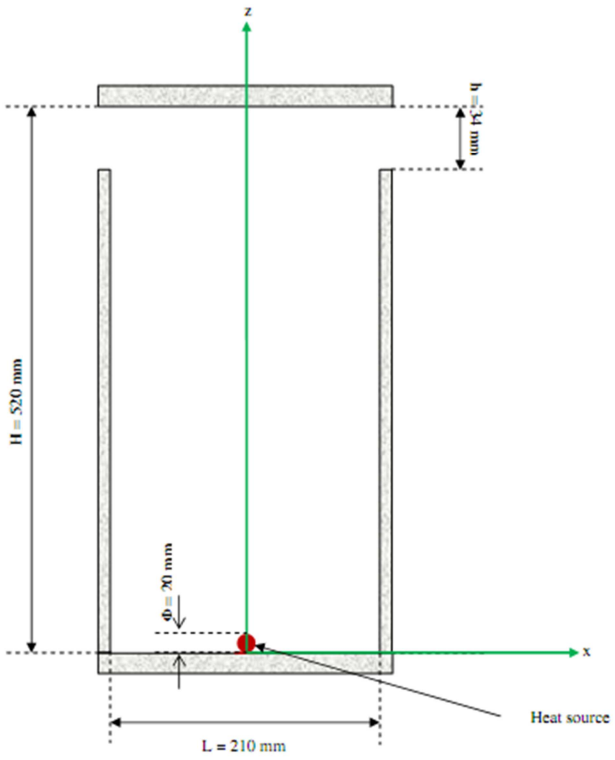

Figure 1. *Numerical device.*

3. Mathematical Formulation and Numerical Methods

3.1. Mathematical Formulation

To solve the conservation equations of mass, momentum and energy, and obtain a more representative mathematical

model of the physical problem studied, we considered that the regime is permanent. The Newtonian fluid is compressible. The temperature of the heat source is constant over time. Heat transfer by radiation is negligible. The physical properties of the fluid are constant except for the density obeying the Boussinesq approximation. And the dissipated power density is negligible.

The conservation equations of mass (1), momentum (2) and energy (3) are as follows [2]:

$$\rho\left(\frac{\partial u}{\partial x}+\frac{\partial v}{\partial y}+\frac{\partial w}{\partial z}\right)=0 \quad (1)$$

$$\begin{cases} u\frac{\partial u}{\partial x}+v\frac{\partial u}{\partial y}+w\frac{\partial u}{\partial z}=-\frac{1}{\rho}\frac{\partial P}{\partial x}+\nu\left(\frac{\partial^2 u}{\partial x^2}+\frac{\partial^2 u}{\partial y^2}+\frac{\partial^2 u}{\partial z^2}\right) \\ u\frac{\partial v}{\partial x}+v\frac{\partial v}{\partial y}+w\frac{\partial v}{\partial z}=-\frac{1}{\rho}\frac{\partial P}{\partial y}+\nu\left(\frac{\partial^2 v}{\partial x^2}+\frac{\partial^2 v}{\partial y^2}+\frac{\partial^2 v}{\partial z^2}\right) \\ u\frac{\partial w}{\partial x}+v\frac{\partial w}{\partial y}+w\frac{\partial w}{\partial z}=-\frac{1}{\rho}\frac{\partial P}{\partial z}+\nu\left(\frac{\partial^2 w}{\partial x^2}+\frac{\partial^2 w}{\partial y^2}+\frac{\partial^2 w}{\partial z^2}\right)-g\beta(T-T_{ext}) \end{cases} \quad (2)$$

$$u\frac{\partial T}{\partial x}+v\frac{\partial T}{\partial y}+w\frac{\partial T}{\partial z}=\alpha\left(\frac{\partial^2 T}{\partial x^2}+\frac{\partial^2 T}{\partial y^2}+\frac{\partial^2 T}{\partial z^2}\right) \quad (3)$$

With

$$\frac{\partial P}{\partial z}=\frac{\partial(P'-P_0)}{\partial z} \quad (4)$$

$$P_0=P_{0i}-\rho_0 gz \quad (5)$$

$$P'=P_i'-\rho gz \quad (6)$$

$$\frac{\partial P_0}{\partial z}=-\rho_0 gz \quad (7)$$

$$\frac{\partial P'}{\partial z}=-\rho gz, \frac{\partial(P'-P_0)}{\partial z}=(\rho_0-\rho) \quad (8)$$

Where the meanings of the following quantities are identical to that of Koueni Toko *et al.* [3],

P_0: Pressure outside of the enclosure;

$\rho_0=1{,}2\ kg.m^{-3}$: Density of air outside the enclosure; It has been determined for a reference temperature of 300K;

P': Pressure at the interior in the enclosure;

ρ: Density of the air inside the enclosure;

$g\beta(T-T_{ext})$: Buoyancy force generated by the heat source. This force varies because the local temperature varies.

x+, y+, z+, u+, v+, w+ T+ et *P+* represente the grandeurs without dimension [2].

u, v and w represent the components of the velocity along the x, y and z directions.

The momentum conservation equations are established by considering that $\frac{\rho_\infty}{\rho}\approx 1$ and that the density variations over time and space are negligible [2]. Therefore, the momentum conservation equations established for a stationary Newtonian compressible fluid is similar to the momentum conservation equations for a stationary Newtonian incompressible fluid. These momentum and energy conservations equations are represented by Equations (2) and (3) [2].

$$x^+=\frac{x}{L}, y^+=\frac{y}{L}, z^+=\frac{z}{H}, u^+=\frac{u}{U_0}, v^+=\frac{v}{U_0},$$

$$w^+=\frac{w}{U_0}, T^+=\frac{T-T_{ext}}{T_0-T_{ext}}, \text{ et } P^+=\frac{P}{|P_{max}|}$$

With

$$U_0=\sqrt{\frac{P_{max}}{\rho_\infty}} \quad (9)$$

U_0 is the maximum cool air entering the enclosure.

According to Koueni Toko *et al.* [3],

$\delta=\frac{\mathrm{L}}{\mathrm{H}}=\frac{1}{2{,}476}$: The inverse of aspect ratio;

$Gr=\frac{g\beta H^3(T_0-T_{ext})}{\nu^2}$: The Grashof number;

$Gr^*=\delta^2 Gr$: The Grashof number reduced.

$Ra^*=\delta^2 Ra$: The Rayleigh number reduced;

$Pr=\frac{\nu}{\alpha}$: The Prandtl number.

The conservation equations of mass (10), momentum (11) and energy dimensionless (12) are as follows [2]:

$$\rho\left(\frac{1}{\delta}\frac{\partial u^+}{\partial x^+}+\frac{1}{\delta}\frac{\partial v^+}{\partial y^+}+\frac{\partial w^+}{\partial z^+}\right)=0 \quad (10)$$

$$\begin{cases} \frac{u^+}{\delta}\frac{\partial u^+}{\partial x^+}+\frac{v^+}{\delta}\frac{\partial u^+}{\partial y^+}+w^+\frac{\partial u^+}{\partial z^+}=-\frac{1}{\delta}\frac{\partial P^+}{\partial x^+}+\frac{1}{Gr^{*1/2}}\left(\frac{\partial^2 u^+}{\partial x^{+2}}+\frac{\partial^2 u^+}{\partial y^{+2}}+\delta\frac{\partial^2 u^+}{\partial z^{+2}}\right) \\ \frac{u^+}{\delta}\frac{\partial v^+}{\partial x^+}+\frac{v^+}{\delta}\frac{\partial v^+}{\partial y^+}+w^+\frac{\partial v^+}{\partial z^+}=-\frac{1}{\delta}\frac{\partial P^+}{\partial y^+}+\frac{1}{Gr^{*1/2}}\left(\frac{\partial^2 v^+}{\partial x^{+2}}+\frac{\partial^2 v^+}{\partial y^{+2}}+\delta\frac{\partial^2 v^+}{\partial z^{+2}}\right) \\ \frac{u^+}{\delta}\frac{\partial w^+}{\partial x^+}+\frac{v^+}{\delta}\frac{\partial w^+}{\partial y^+}+w^+\frac{\partial w^+}{\partial z^+}=-\frac{1}{\delta}\frac{\partial P^+}{\partial z^+}+\frac{1}{Gr^{*1/2}}\left(\frac{\partial^2 w^+}{\partial x^{+2}}+\frac{\partial^2 w^+}{\partial y^{+2}}+\delta\frac{\partial^2 w^+}{\partial z^{+2}}\right)-T^+ \end{cases} \quad (11)$$

$$\frac{u^+}{\delta}\frac{\partial T^+}{\partial x^+}+\frac{v^+}{\delta}\frac{\partial T^+}{\partial y^+}+w^+\frac{\partial T^+}{\partial z^+}=\frac{1}{(PrRa^*)^{1/2}}\left(\frac{\partial^2 T^+}{\partial x^{+2}}+\frac{\partial^2 T^+}{\partial y^{+2}}+\delta\frac{\partial^2 T^+}{\partial z^{+2}}\right) \quad (12)$$

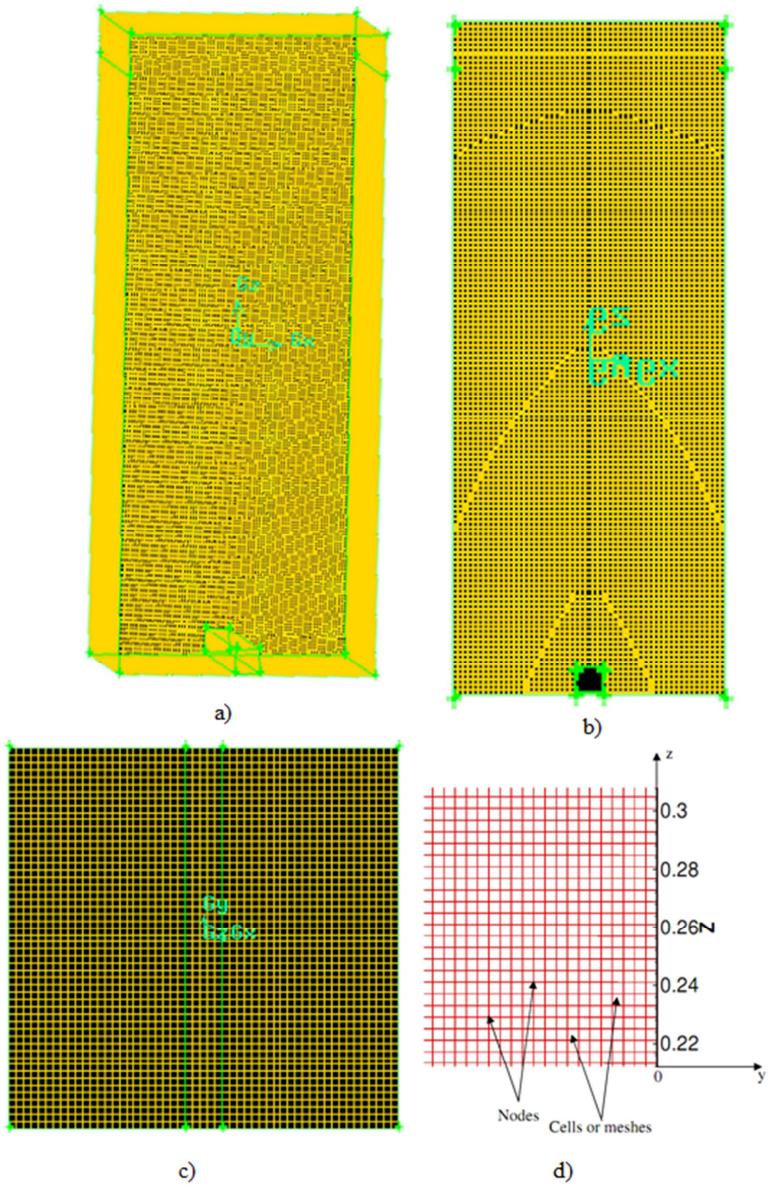

Figure 2. *Numerical mesh device a) view 3D, b) view 2D (z; x) c) view 2D (y; x) d) view 2D (z; y).*

3.2. Numerical Methods

We used direct numerical simulation (DNS) to solve the conservation equations of mass (10), momentum (11) and energy (12). This DNS is based on the finite volume method. We used this DNS because the thermal plume is created by a cylindrical heat source at temperature ΔT0. The thermal plume is assumed to be turbulent. The discretization of these conservation equations using the QUICK scheme given by Leonard [17], gives a system of algebraic equations whose solution makes it possible to obtain all the variables of the problem studied. This resolution method was developed by Patankar [18]. For pressure resolution and correction, we used the Weighted Body Strength scheme and the SIMPLE algorithm developed by Spalding and Patankar. Numerical calculations were performed using the commercial computer code FLUENT. In this code, the iterative computation is performed by the Gauss Seidel linear system solving algorithm in conjunction with the AMD algebraic multigrid method to solve the resulting system.

The conservation equations of the studied problem are solved in steady state by considering the walls of the non-adiabatic enclosure and by using a fine non-uniform regular mesh of the numerical device. This mesh was chosen to reduce the calculation errors, to have a rapid convergence and a stable result approaching reality. Three meshes with different number of meshes (89001 meshes, 366654 meshes and 482328 meshes) were used (Table 2) in order to determine for the resolution of the problem, the mesh which gives the optimal solution which must be independent of the density of the mesh for be sure of the realism of the solution given by the solver after convergence. This is to maintain a good Quality of the elements, to ensure a good Resolution in the regions with a strong gradient, to ensure a good Smoothing in the transition zones between the parts with fine mesh, the parts with less coarse mesh and the parts with coarse mesh; minimize the

Total number of elements (reasonable computation time). From Table 4, it appears that mesh 2 of 366654 meshes is the optimal mesh. Mesh 2 is shown in Figure 2.

The cylindrical shape with a square base section of the heat source as well as the square shape of the openings allow good smoothing, minimize distortions, have good convergence, reduce calculation time and ensure good resolution in regions with strong temperature gradients.

Table 1. *Values of the Rayleigh number reduced depending ΔT_0.*

ΔT_0 (K)	25	40	60
Ra*	6.09×10^7	9.74×10^7	1.61×10^8

Table 2. *Characteristics of Numerical devise meshes.*

Meshes	Mesh 1	Mesh 2	Mesh 3
Cells	89001	366654	482328
Nodes	95812	384048	503270

Table 3. *Static pressure differential values $|P_{max}|$ and temperature differential values ΔT depending to the number of mesh of geometry studied for ΔT_0 = 60 K.*

Meshes		Mesh 1	Mesh 2	Mesh 3
Temperature differential	Z+ = 0.1	6.16	7.534	6.919
	Z+ = 0.3	6.952	10.675	7.912
	Z+ = 0.6	7.895	8.875	10.268
	Z+ = 0.9	7.757	9.525	8.396
Static pressure differential	Z+ = 0.1	-0.13	-0.166	-0.157
	Z+ = 0.3	-0.104	-0.135	-0.127
	Z+ = 0.6	-0.066	-0.076	-0.074
	Z+ = 0.9	-0.015	-0.017	-0.017

Table 4. *Maximum static pressure differential values $|P_{max}|$ depending on the temperature of the heat source ΔT_0.*

ΔT_0 (K)	25	40	60
$\|P_{max}\|$ (Pa) numerical device of this study	0,0865	0,1396	0,1973
$\|P_{max}\|$ (Pa) Experimental device	0.2	0.4	0.4

3.3. Boundary Conditions

The enclosure is placed in a large closed room with very low flux air renewal. The room is not ventilated. We put ourselves in the same experimental conditions as those of Koueni Toko [2]. Before heating begins, the enclosure is balanced with the interior of the room. Therefore, we assume that the total pressure difference (ΔP) between the inside and the outside of the enclosure is zero. There is no air entering the enclosure. To solve the conservation equations of mass (10), momentum (11) and energy (12) we used the boundary conditions at the walls of the enclosure for each quantity studied (temperature, pressure and velocity).

These boundary conditions are shown in Figure 3.

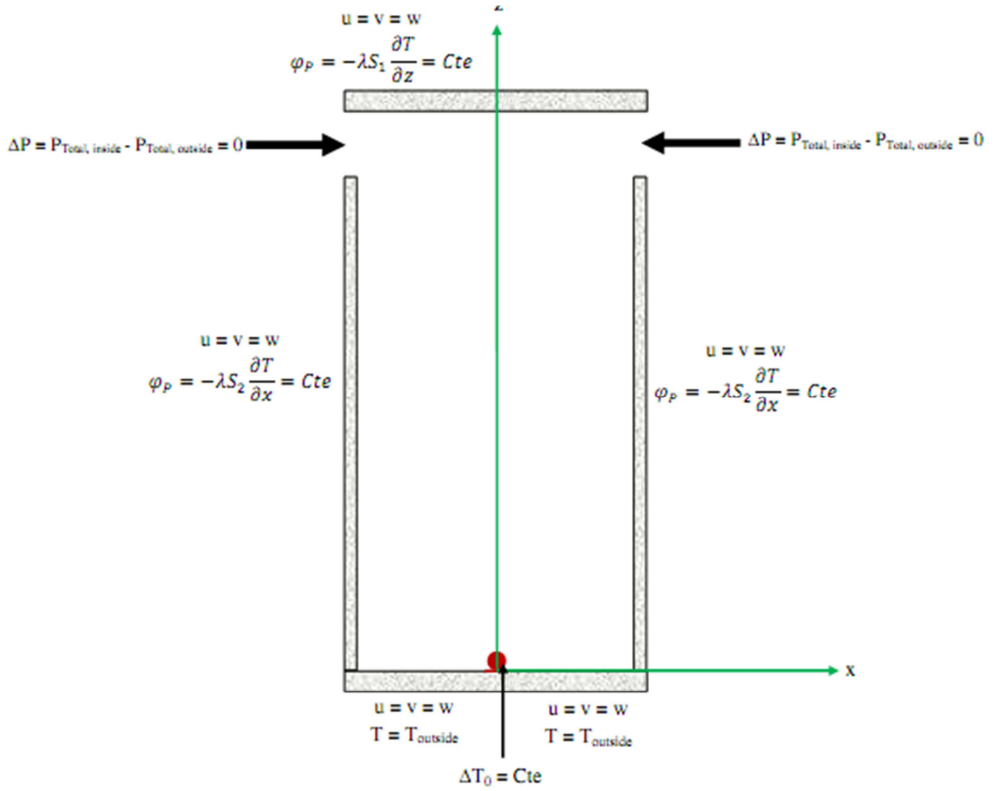

Figure 3. *Boundary condition.*

Figure 3 show that at the side walls and the ceiling we have a Newman condition. That is, $\varphi_p = cte$ the heat flow which passes through each side wall and the ceiling. The expression of φ_p given by the following equation (13).

$$\varphi_p = -\lambda S \frac{\partial T}{\partial x} = cte = h_i S(T_p - T_\infty) = h_o S(T_p - T_\infty) \quad (13)$$

The velocity values are zero at the walls.

$$P_{total} = P_{stat} + \rho\frac{V^2}{2g} + \rho gz \quad (14)$$

$$\Delta P = P_{total,inside} - P_{total,outside} \quad (15)$$

$$S_1 = L \times l \quad (16)$$

$$S_2 = (H - h) \times l \quad (17)$$

4. Results and Discussion

The fields and the temperature profiles and the differential static pressure profiles obtained by numerical calculation as a function of the reduced Rayleigh number (Ra^*) in the enclosure in steady state will be presented in this part. These values of Gr* as a function of the values of ΔT0 are presented in table 1. We note that the reduced Rayleigh number is greater than 10^9. This result makes it possible to consider that the thermal plume generated by the heat source in the containment is turbulent.

The differential static pressure profiles obtained by numerical calculations and in steady state will be compared with experimental measurements from the literature.

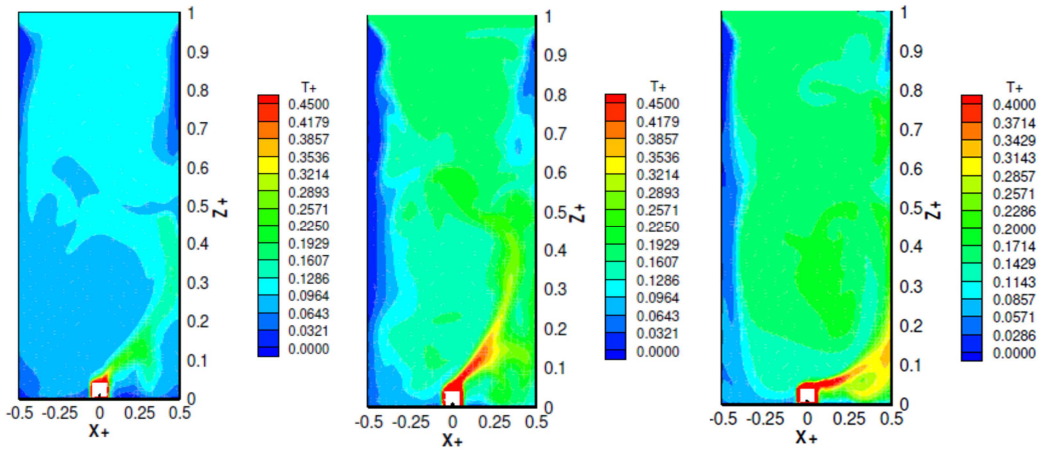

a) b) c)

Figure 4. *Temperature fields obtained numerically at the position y+= 0, a) Ra* = 6.09×10⁷, b) Ra* = 9.74×10⁷, c) Ra* = 1.61×10⁸.*

4.1. Influence of the Reduced Raleigh Number on the Thermal Fields

Numerical temperature fields in steady state, at position y+ = 0 and for reduced Rayleigh numbers of 6.09×10^7, 9.74×10^7 and 1.61×10^8. are represented Figure 4. This figure shows that, the thermal plume strongly inclined towards the right wall of the enclosure, reaches the ceiling where it is destroyed by shearing. At the top of the openings the air is warm and at the bottom the air is cool. From z+ = 0.5 on the enclosure ceiling and outside the side walls, the temperature is almost homogeneous in the enclosure. The temperature at the top of the openings increases with the reduced Rayleigh number.

4.2. Influence of Reduced Raleigh Number on Dimentionless Temperature Profiles

The Figure 5 represents the dimensionless temperature profiles, in steady state, obtained at the position y+ = 0 depending on the reduced Rayleigh numbers of 6.09×10^7, 9.74×10^7 and 1.61×10^8. At position x+ = 0, the temperature in the enclosure decreases from the heat source to position z+ = 0.08. From this position on the ceiling of the enclosure she faintly believes. At positions x+ = - 0.25 and 0.25, the temperature in the enclosure increases from floor to ceiling. At position z+ = 0.08 on the ceiling of the enclosure and at positions x+ = - 0.25, 0, 0.25, the temperature is constant in the enclosure. At position x+ = - 0.5, the temperature is lower in the floor enclosure at position z+ = 0.97. At this height of the enclosure and at position x + = 0.5, the temperature fluctuates. From the position z+ = 0.97 on the ceiling of the enclosure, the temperature is almost identical to that of the positions x+ = - 0.25, 0, 0.25.

4.3. Influence of Reduced Raleigh Number on Differential Static Pressure

Figure 6 shows the numerical differential static pressure profiles, in steady state, at the position y+ = 0 depending on the reduced Rayleigh numbers of 6.09×10^7, 9.74×10^7 and 1.61×10^8. This Figure shows that, the values of the differential static pressure are negative in the enclosure of the floor at the position z+ = 0.97. From the latter position on the ceiling of the enclosure they are positive. These differential static pressure values grow from the floor to the ceiling of the enclosure and are almost constant from the position x+ = - 0.5 to the position x+ = 0.5. The profiles of the differential static pressure in the enclosure are comparable to oblique lines of slopes varying with the reduced Rayleigh number. These results also show that hot air exits the enclosure from the top of the openings and cool air enters the enclosure from the bottom.

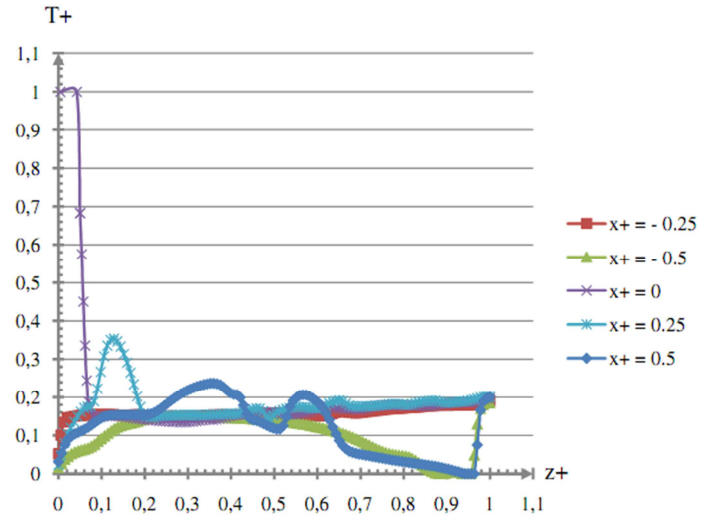

a)

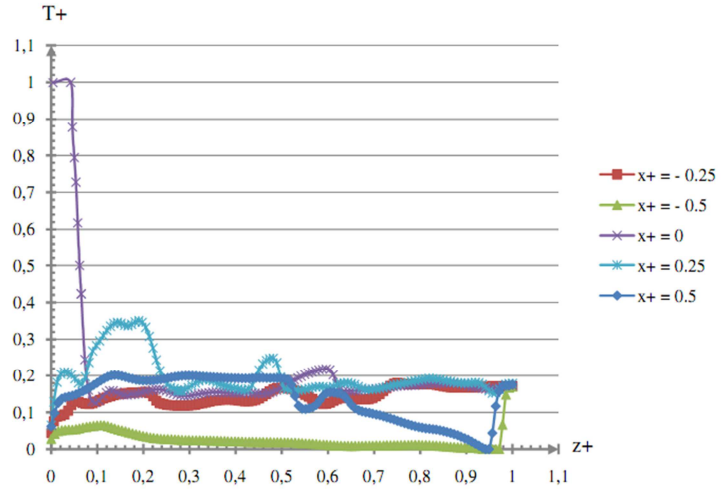

b)

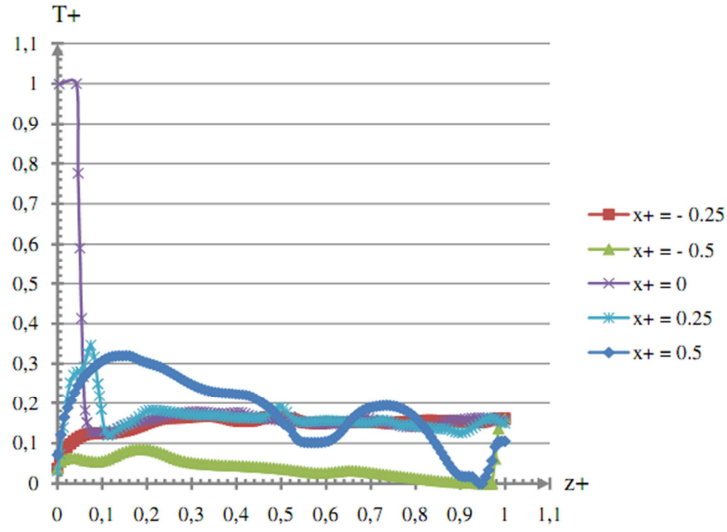

c)

Figure 5. *Dimensionless differential temperature vertical profiles obtained numerically at positions x+ = - 0.5, - 0.25, 0: 0.25, 0.5 and y+ = 0, a) Ra* = 6.09×10^{7}, b) Ra* = 9.74×10^{7}, c) Ra* = 1.61×10^{8}.*

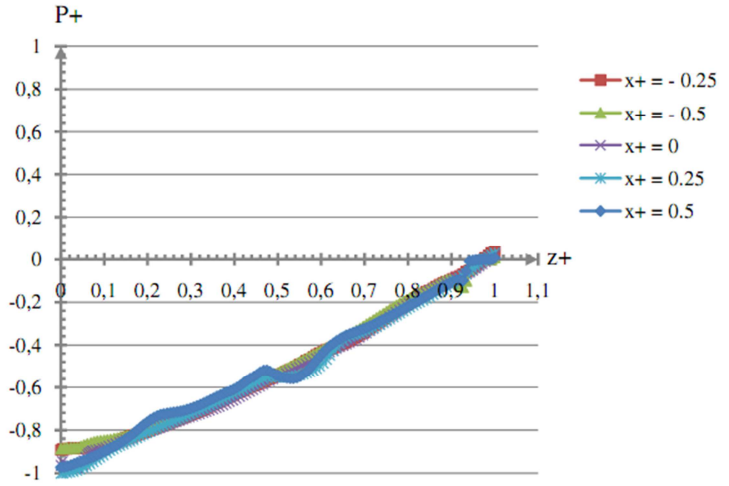

a)

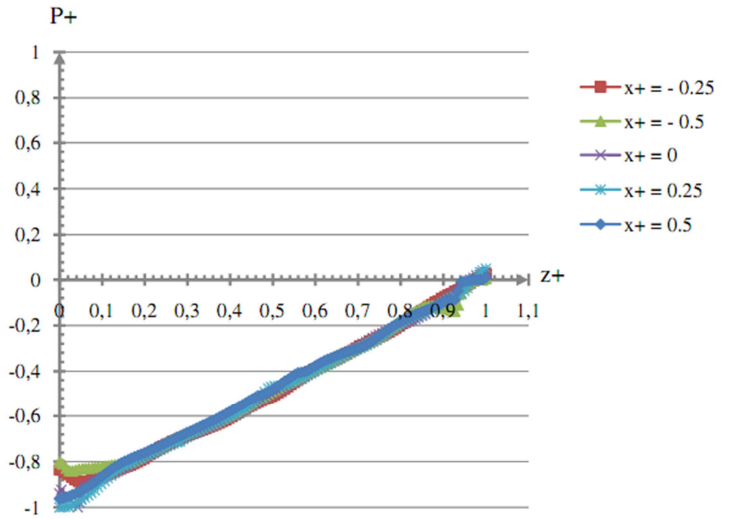

b)

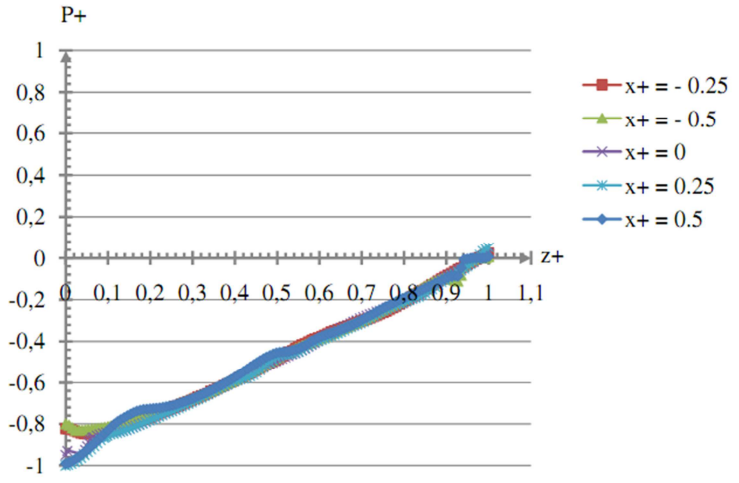

c)

Figure 6. *Dimensionless differential pressure static vertical profiles obtained numerically at positions x+ = - 0.5, - 0.25, 0: 0.25, 0.5 and y+ = 0, a) Ra* = 6.09×10^{7}, b) Ra* = 9.74×10^{7}, c) Ra* = 1.61×10^{8}.*

4.4. Comparison of Differential Static Pressure Obtained by Numerical Calculation with Those of the Experimental Measurements

Figure 7 represents the comparison of the profiles of differential static pressure obtained by experiment and by numerical calculations, in stationary mode, at the position y+ = 0 depending on the reduced Rayleigh numbers of 6.09×10^{7}, 9.74×10^{7} and 1.61×10^{8}. This Figure shows that the results obtained by numerical calculations and by experiment agree.

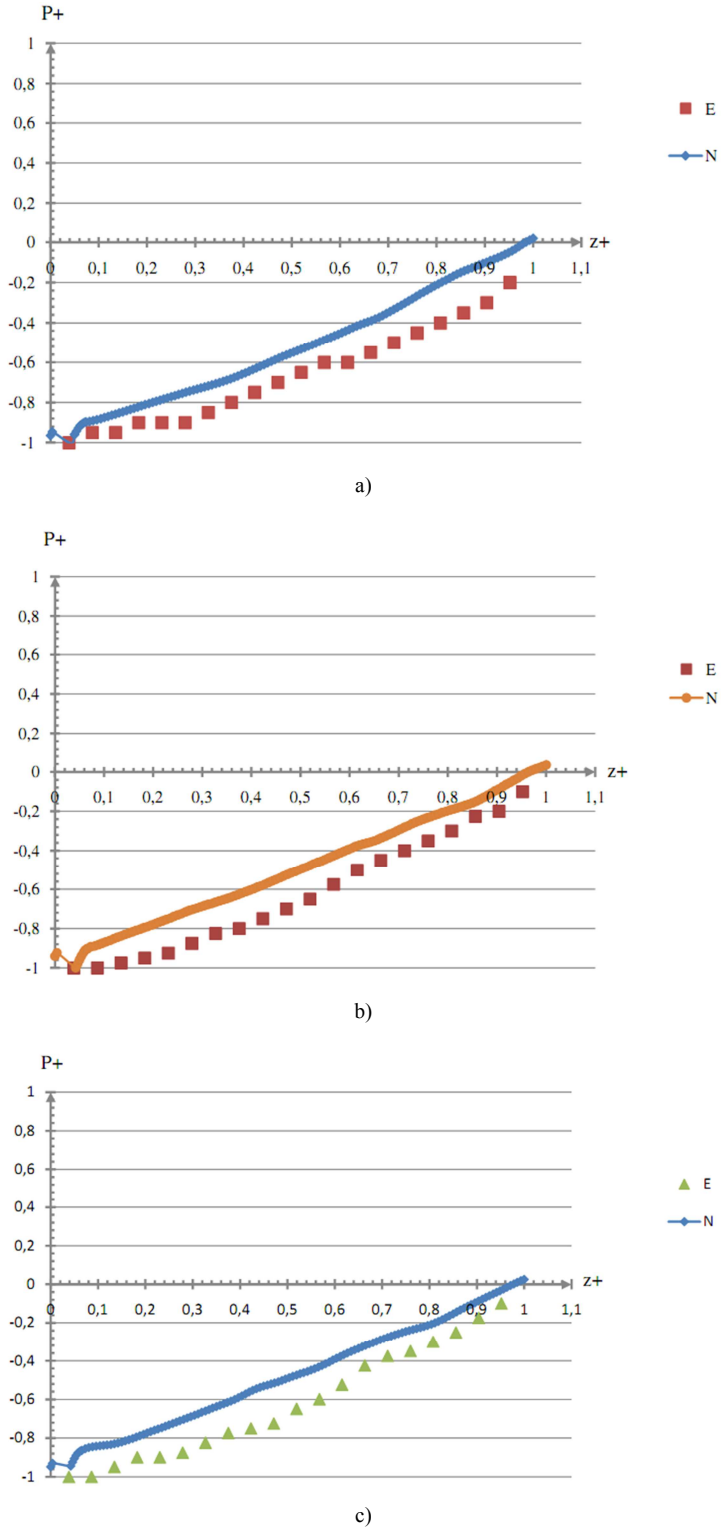

Figure 7. *Comparison of dimensionless differential pressure static vertical profiles obtained numerically with of experimental at positions y+ = 0, a) Ra* = 6.09×10^{7}, b) Ra* = 9.74×10^{7}, c) Ra* = 1.61×10^{8}.*

5. Conclusion

At the end of this work on the study of thermal fields in a semi-ventilated enclosure heated by a linear heat source, it is found that the air movements are governed in the enclosure by the thermal plume. The thermal plume is generated by a linear heat source with a diameter of 20 mm and a length of 200 mm placed at the position x + = 0 and at 2 mm from the floor, which creates a thermal gradient in the enclosure and air movements at the bottom. openings (Figure 6). This plume is held in the enclosure by the force of the buoyancy. The semi-ventilated enclosure, 520 mm high, 210 mm wide and 210 mm long, has two openings located in the ceiling of the enclosure on both side walls. The openings have a height of 34 mm and a length of 210 mm. The experimental measurements of the differential static pressure were carried out using the FC014 micro-manometer and the numerical calculations of the thermal fields and the differential static pressure using the DNS method. The simulation technique is based on the finite volume method. The study was carried out under a steady-state regime. The results from numerical calculations show that the thermal plume inclined towards the right wall of the enclosure (Figure 4) reaches the ceiling where it is destroyed by shearing and the hot air leaves the enclosure through the top of the openings (Figure 6). Cool air enters the enclosure through the bottom of the openings (Figures 5 and 6), descends to the floor near the side walls (Figure 4), where it mixes with the warm air in the enclosure. The hot gas outlet temperature of the enclosure increases with increasing reduced Rayleigh number. The comparison of the results of numerical calculations with those of the experiment agrees.

In perspective, we will carry out this study in unsteady state for several positions of the heat source in order to elucidate the phenomena occurring in this type of enclosure.

Nomenclature

Lowercase

l	Width Enclosure, m
x	Longitudinal coordinate, m
y	Vertical coordinate, m
z	Transverse coordinate, m
u	Horizontal component of the velocity, $m.s^{-1}$
v	Vertical component of the velocity, $m.s^{-1}$
w	Transverse velocity component, $m.s^{-1}$
cte	Constant
h_i	Heat exchange coefficient inside the enclosure, $W.m^{-1}.K^{-1}$
h_o	Heat exchange coefficient outside the enclosure, $W.m^{-1}.K^{-1}$

Capital Letters

L	Enclosure length, m
H	Enclosure height, m
ΔT_0	Temperature difference between the heat source and the outside, K
T	Temperature inside the enclosure, K
T_0	Temperature of the heat source, K
U_0	Maximum inlet gas velocity in the enclosure, K
P	Static pressure inside enclosure, Pa
P_{max}	Maximum static pressure inside enclosure, Pa
P_{total}	Total pressure, Pa
$P_{total,\ inside}$	Total pressure inside the enclosure, Pa
$P_{total,\ outside}$	Total pressure outside the enclosure, Pa
$T_{outside}$	Temperature outside the enclosure, K
T_p	Side wall or ceiling temperature, K
T_∞	Temperature away from side wall or ceiling inside or outside the enclosure, K
S_1	Section of the enclosure ceiling, m^2
S_2	Section of the side walls of the enclosure, m^2

Greek Symbols

ν	Kinematic viscosity of air, $m^2.s^{-1}$
ρ	Density, $kg.m^{-3}$
β	Coefficient of thermal expansion, K^{-1}

ρ_{ext}	Density of gases outside of the enclosure, $kg.m^{-3}$
φ_p	Heat flux to the side walls and ceiling of the enclosure, $W.m^{-1}$
λ	Thermal conductivity of the walls in Plexiglas, $W.m^{-1}.K^{-1}$

Dimensionless Numbers

Ra	Rayleigh number
Pr	Prandtl number
Gr	Grashof number

Special Characters

Ra*	Reduced Rayleigh number
Gr*	Reduced Grashof number
x+	Dimensionless longitudinal coordinate
y+	Dimensionless vertical coordinate
z+	Coordinated transverse to size
u+	Horizontal component of the dimensionless speed
v+	Vertical component of the dimensionless speed
w+	Transverse component of the dimensionless speed
P+	Static pressure to size
T+	Temperature to size
δ	Aspect Ratio

References

[1] Baines W. D., Turner J. S. (1969) Turbulent buoyant convection from a source in a confined region, *Journal of Fluid Mechanics*, 37, 51-80.

[2] Koueni Toko C. A. (2019) Etude des champs dynamique et thermique dans une enceinte semi-ventilée en convection naturelle, *Rapport annuel de thèse-CORIA*.

[3] Kouéni-Toko C. A., Tcheukam-Toko D., Kuitche A., Patte-Rouland B., Paranthoën P. (2020) Numerical modeling of the temperature fields in a semi-confined enclosure heated by a linear heat source, *International Journal of Thermofluids, 100017* https://doi.org/10.1016/j.ijft.2020.100017

[4] Fitzgerald S. D. and Woods A. W. (2010) Transient natural ventilation of a space with localized heating, *Building and Environment*, 45 2778-2789.

[5] Jeremy C. P. and Andrew W. W. (2004), On ventilation of a heated room through a single doorway, *Building and Environment,* 39 241-253.

[6] Paranthoën P. and Gonzalez M. (2010), Mixed convection in a ventilated enclosure, *International Journal of Heat and Fluid Flow,* 31 172-178.

[7] Linden P. F., Lane-Serff G. F., Smeed D. A. (1990) Emptying filling boxes: the fluid mechanics of natural ventilation, *Journal of Fluid Mechanics*, 212, 309–335.

[8] Kaye N. B. and Hunt G. R. (2004) Time-dependent flows in an emptying filling box, *Journal of Fluid Mechanics, 520, 135-156.*

[9] Gladstone C. and Woods A. W. (2001) On buoyancy-driven natural ventilation of a room with a heated floor, *Journal of Fluid Mechanics*, 441, 293-314.

[10] Kaye N. B., Hunt G. R. (2007) Overturning in a filling box, *Journal of Fluid Mechanics*, 576, 297-323.

[11] Jilani G., Jayaraj S., Khadar K. (2002) Numerical analysis of free convective flows in partially open enclosure, Heat and Mass Transfer, 38, 261-270.

[12] Yu E., Yoshi Y. (1997) A numerical study of three-dimensional laminar natural convection in a vented enclosure, International Journal of Heat and Fluid Flow, 18, 6, 800-812.

[13] Fitzgerald S. D., Woods A. W. (2004) Natural ventilation of a room with vents at multiple levels, Building and Environment, 39, 505-521.

[14] Andersen K. T. (1995) Theoretical considerations on natural ventilation by thermal buoyancy, Proceedings ASHRAE, San Diégo USA.

[15] Kouéni Toko Christian Anicet. Numerical Simulation of the Velocity Fields Generated by a Plume in Enclosure with Several Openings. International Journal of Fluid Mechanics & Thermal Sciences. Vol. 7, No. 4, 2021, pp. 53-67. doi: 10.11648/j.ijfmts.20210704.11.

[16] Kouéni-Toko Christian Anicet, Patte-Rouland Béatrice, Paranthoën Pierre. Experimental Study of the Pressure Generated by a Linear Heat Source in a Semi–ventilated Enclosure. Engineering and Applied Sciences. Vol. 7, No. 1, 2022, pp. 8-15. doi: 10.11648/j.eas.20220701.12.

[17] Leonard, B. P. (1979) A stable and accurate convective modeling procedure based on quadratic interpolation, *Comput methods Appl. Mech. Eng., 19, 59-98.*

[18] Patankar S. V. (1980) Numerical heat transfert and fluid flow, *Hemisphere Publishing Corporation.*